International Journal of Thermophysics, Vol. 4, No. 1, 1983

Thermal Conductivity Measurement of n-Butane Over Wide Temperature and Pressure Ranges

C. A. Nieto de Castro,[1] R. Tufeu,[2] and B. Le Neindre[2]

Received December 8, 1982

The thermal conductivity of n-butane has been measured by a coaxial-cylinder method over a pressure range from 0.1 MPa up to 70 MPa and a temperature range from room temperature to 600 K, covering all fluid states. The estimated accuracy of the method is about 2%. Special emphasis has been given to the behavior of the thermal conductivity near the critical point, and the critical enhancement has been studied for $3.6\ \text{K} < \Delta T < 176\ \text{K}$. The effect of inelastic collisions upon transport properties of the dilute gas has been discussed. The results obtained for the reduced critical enhancement as a function of the reduced critical temperature confirm the universality of the critical exponent, for the n-alkanes, whereas the reduced excess thermal conductivity outside the critical region is a function of the reduced density and of the n-alkane.

KEY WORDS: butane; corresponding states; critical region; thermal conductivity.

1. INTRODUCTION

Hydrocarbons are very important fluids in the chemical process industry, namely, in petroleum refining and petrochemical plants. They are also a very sensible series of substances to study and develop corresponding states of transport properties. As part of an extensive program to study transport properties of fluids from room temperature up to 600 K and pressures up to 70 MPa, we have measured the thermal conductivity of n-butane. Comparison with results formerly obtained for methane, ethane, propane, and isobutane led us to study the behavior of the thermal conductivity of these

[1] Departamento de Química, FCUL, Centro de Química Estrutural, Complexo I, 1096 Lisboa Codex, Portugal.
[2] LIMHP, CNRS, Université Paris-Nord, 93430 Villetaneuse, France.

0195-928X/83/0300-0011$03.00/0

polyatomic fluids in the critical region, in order to obtain evidence for universal behavior near the critical point.

Measurements of the thermal conductivity of n-butane are few, covering the dilute gas zone [1–3] and the liquid zone [2, 4, 5] as a function of density. Measurements on the saturation line have also been reported [6, 7]. All these data are of limited accuracy ($\pm 5\%$) with the exception of Pittman's data [6], which have an accuracy of $\pm 2\%$. No data on the critical region have been reported so far. In this paper the most extensive study of the thermal conductivity of n-butane to date, covering the subcritical region (298.2 K, 358.2 K, 383.2 K, 413.2 K) and the supercritical region (428.8 K, 431.4 K, 436.0 K, 454.2 K, 480.0 K, 518.2 K, 601.2 K), from 0.1 MPa to 70 MPa, is reported.

2. EXPERIMENTAL PROCEDURE

The method used to measure the thermal conductivity of n-butane was the vertical coaxial-cylinder method, described in detail previously [8, 10]. To determine the thermal conductivity we must know the amount of heat emitted from the inner cylinder. We then measure the voltage difference and the current intensity in the heating element, placed inside the inner cylinder, along its axis. The temperature difference between the outside wall of the inner cylinder and the inner wall of the outside cylinder is obtained with eight Pt/Pt-Rh 10% thermocouples in series, four in each cylinder. The temperature difference is ~ 2 K outside the critical region; there it is about 0.1 to 0.2 K, and it is measured with a precision of 0.003 K. The cell temperature is measured with a thermocouple located in the external cylinder, with an accuracy of 0.1 K.

The cell is set up in a high-pressure vessel heated externally by coils wound on a copper block. High pressures are obtained by a bellow system, using nitrogen from a normal cylinder ($p \sim 150$ bar) and a gas compressor. An auxiliary vessel allows us to condense the fluid at liquid nitrogen temperature, and to reheat the closed vessel to room temperature, when the pressure of the nitrogen bottle is low. The pressure was measured with high accuracy Bourdon gauges manufactured by Heise Company.

The thermal conductivity is obtained from

$$\lambda_m = \frac{W}{\Delta T} K \tag{1}$$

where W is the power dissipated in the inner cylinder ($W = VI$), ΔT is the temperature difference between the two cylinders, and K is the cell con-

stant. This constant has been determined from capacity measurements and is equal to 3.405×10^{-2} m^{-1}. Equation (1) gives an ideal value for the thermal conductivity as the total energy dissipated in the inner cylinder is transmitted mainly by conduction in the fluid, but conduction by the cylinder element itself and radiation are also present. The conduction through the cylinder element, electric leads, and ceramic supports, herein called parallel conduction, λ_p, has been previously estimated as a function of measured thermal conductivity λ_m [8–10], as it is not a function of temperature or pressure, to a first approximation.

The simultaneous heat transfer by radiation and conduction in steady-state concentric cylindrical instruments, containing a medium like a liquid hydrocarbon, has not yet been solved [11], and it is not yet possible to make any sensible correction to the measured thermal conductivities in the dense fluid region. The gas phase and the dense fluid have been considered as transparent fluids. The thermal conductivity of the fluid is then evaluated from

$$\lambda_c = \lambda_m - \lambda_p - \lambda_r \tag{2}$$

where λ_r is the radiative component of the thermal conductivity,

$$\frac{\lambda_r}{\lambda_c} = \frac{Q_r}{Q_c} \simeq \frac{4S\sigma\epsilon T_1^3 \Delta T}{VI} = \alpha \tag{3}$$

where S is the surface of the emitter, ϵ is the emissivity of silver (the cell material), and σ is the Stefan–Boltzmann constant. T_1 is the temperature of the fluid. The ratio α for the present measurements is never greater than 0.007.

Using Eqs. (2) and (3) we obtain

$$\lambda_c = (\lambda_m - \lambda_p)/(1 + \alpha) \tag{4}$$

Measurements were made along an isotherm at decreasing pressures. It is very difficult to maintain the temperature of the cell constant during a pressure scan, owing to changes in the heat conduction of the fluid in the high-pressure vessel. The values of the thermal conductivity were therefore corrected to a nominal temperature using the procedure given in the footnote of Table I. The butane (purity 99.95%) was supplied by Air Liquide, France. For the measurements near the critical point, the pressure range covered was chosen to study in detail the critical enhancement, the high pressure zone being neglected for some intermediate isotherms.

Table I. Thermal Conductivity of n-Butane at $T_{nom} = 298.2$ K

T (K)	P (MPa)	ρ (kg · m^{-3})	$\lambda(T,\rho)$ (mW · m^{-1} · K^{-1})	$\lambda(T_{mon},\rho)$ (mW · m^{-1} · K^{-1})
296.6	50.00	630.19	136.1	136.3
297.0	50.00	629.89	136.2	136.3
297.4	40.20	621.38	130.5	130.6
297.7	30.20	611.77	125.4	125.5
298.2	20.10	600.52	119.4	119.4
298.6	9.990	587.35	112.9	112.9
299.3	1.000	572.63	105.9	105.8
299.7	1.000	572.16	105.8	105.7
298.7	0.180	4.454	16.40	16.36
299.7	0.190	4.698	16.43	16.28

3. RESULTS

The results for the liquid and gas regions are presented in Tables I to IV, for the nominal temperatures 298.2 K, 358.2 K, 383.2 K, and 413.2 K, respectively. The tables include the thermal conductivity at different temperatures and densities $\lambda(T,\rho)$ and the values corrected to the nominal temperatures. These corrections did not exceed 0.5%; therefore, no additional uncertainty is introduced in the data. The values for the liquid state have not been corrected for the interaction between conduction and radiation in participating media, this contribution being estimated to be about 2% in the density range covered. In the absence of an exact treatment for this correction, we decided not to correct for radiation until this theoretical analysis is available.

Table II. Thermal Conductvity of n-Butane at $T_{nom} = 358.2$ K[a]

T (K)	P (MPa)	ρ (kg · m^{-3})	$\lambda(T,\rho)$ (mW · m^{-1} · K^{-1})	$\lambda(T_{nom},\rho)$ (mW · m^{-1} · K^{-1})
356.5	70.00	604.72	128.7	128.9
356.6	60.20	595.94	124.7	124.9
356.9	50.00	585.59	118.8	118.9
357.2	40.10	574.14	114.2	114.3
358.0	30.20	560.33	108.4	108.4
358.2	20.10	543.68	98.46	98.45
358.6	10.00	521.34	92.85	92.80
358.8	1.200	491.55	84.13	84.06
358.0	1.000	24.050	24.50	24.52
359.0	0.300	6.154	23.50	23.46

[a] Note: $\lambda(T_{nom},\rho) = \lambda(\rho,T) + (\partial\lambda/\partial T)_{\rho,T_{nom}}(T_{nom} - T)$ with $(\partial\lambda/\partial T)_{\rho,T_{nom}} = (d\lambda(0,T)/dT)_{T_{nom}}$

Table III. Thermal Conductivity of n-Butane at $T_{nom} = 383.2$ K

T (K)	P (MPa)	ρ ($kg \cdot m^{-3}$)	$\lambda(T, \rho)$ ($mW \cdot m^{-1} \cdot K^{-1}$)	$\lambda(T_{nom}, \rho)$ ($mW \cdot m^{-1} \cdot K^{-1}$)
386.3	60.00	575.38	117.1	116.7
386.1	50.00	564.24	112.2	111.8
386.0	40.00	551.22	107.6	107.3
385.9	30.00	535.58	101.3	101.0
386.6	28.50	532.27	100.5	100.1
385.7	20.20	516.16	94.93	94.07
386.6	10.10	485.93	86.22	85.78
385.6	10.10	486.91	85.46	85.15
382.1	5.070	470.73	81.17	81.31
385.1	5.000	465.19	79.68	79.43
382.4	3.040	458.20	78.93	79.05
382.7	2.530	453.97	78.00	78.06
382.7	2.030	450.10	77.51	77.57
382.9	1.600	39.234	29.66	29.70
383.1	1.010	21.537	28.03	28.04
383.2	0.460	8.954	27.29	27.29

Table IV. Thermal Conductivity of n-Butane at $T_{nom} = 413.2$ K

T (K)	P (MPa)	ρ ($kg \cdot m^{-3}$)	$\lambda(T, \rho)$ ($mW \cdot m^{-1} \cdot K^{-1}$)	$\lambda(T_{nom}, \rho)$ ($mW \cdot m^{-1} \cdot K^{-1}$)
414.0	68.90	566.58	117.2	117.1
414.1	60.40	557.10	112.6	112.5
414.1	50.60	544.78	108.5	108.4
414.2	40.10	529.09	101.9	101.8
414.2	30.20	510.83	93.79	93.68
414.3	20.00	485.49	87.99	87.89
414.4	10.10	445.52	78.16	78.09
414.5	8.190	433.12	75.97	75.90
411.0	7.130	431.70	76.73	77.00
411.1	5.895	421.63	74.50	74.75
411.1	5.035	411.47	72.81	73.06
411.1	3.995	396.57	71.12	71.38
411.1	3.500	386.71	69.50	69.75
411.1	3.310	382.03	69.16	69.41
411.1	3.105	376.03	68.77	69.02
412.0	2.720	74.153	36.88	36.99
412.4	2.505	63.166	35.55	35.65
412.8	2.000	44.486	34.06	34.11
412.9	1.495	30.424	32.18	32.24
413.1	0.995	18.865	31.59	31.60
413.3	0.495	8.843	30.78	30.77

Table V. Thermal Conductivity of n-Butane Near $T_{nom} = 428.8$ K ($\Delta T = 3.6 \pm 0.1$ K)

T (K)	P (MPa)	ρ (kg · m^{-3})	$\lambda(T, \rho)$ (mW · m^{-1} · K^{-1})
431.3	60.40	545.70	112.1
431.5	50.50	532.24	106.3
432.0	40.00	514.91	100.3
432.3	30.05	494.31	93.98
432.3	20.20	466.50	86.84
432.8	14.97	444.67	81.16
432.8	10.05	414.53	75.12
428.7	6.970	391.68	71.66
428.8	6.520	385.00	69.42
428.8	5.150	366.09	68.24
428.8	5.015	352.12	66.38
428.8	4.500	328.78	65.04
428.8	4.150	289.17	70.08
428.9	4.120	278.28	73.74
428.9	4.085	263.49	76.37
428.9	4.070	254.59	81.03
428.9	4.060	247.54	82.19
428.8	4.050	245.27	85.44
428.8	4.040	236.89	87.12
428.9	4.030	222.08	87.60
428.8	4.020	218.52	85.88
428.8	4.010	209.07	82.56
428.8	4.000	200.12	78.05
428.8	3.990	192.17	73.98
428.8	3.980	185.32	71.10
428.9	3.970	176.92	66.59
429.0	3.960	170.28	62.02
429.1	3.900	150.68	53.95
429.3	3.500	101.72	43.16
431.5	0.990	17.659	35.74

Tables V to XI present the values obtained in the supercritical region, for the nominal temperatures of 428.8 K, 431.4 K, 436.0 K, 454.2 K, 480.0 K, 518.2 K, and 601.2 K, respectively; for different temperatures and pressures; together with the values corrected for nominal temperatures only far from the critical region. This is because the critical enhancement is strongly density and temperature dependent. All the thermal conductivity values in the supercritical region have been corrected for radiation, considering the fluid as transparent and using Eq. (4). The densities reported here were obtained using the NBS equation of state for n-butane [13], some uncertainty being possible in the critical region.

Table VI. Thermal Conductivity of n-Butane Near $T_{nom} = 431.4$ K ($\Delta T = 6.2 \pm 0.1$ K)

T (K)	P (MPa)	ρ (kg · m^{-3})	$\lambda(T, \rho)$ (mW · m^{-1} · K^{-1})
431.40	6.970	384.83	71.24
431.50	6.005	367.68	68.89
431.40	5.005	338.62	67.05
431.40	4.705	322.60	65.95
431.30	4.600	315.64	66.65
431.30	4.500	306.26	66.63
431.30	4.450	300.38	67.32
431.21	4.400	294.59	67.61
431.23	4.350	285.57	68.70
431.27	4.330	280.58	69.67
431.27	4.310	275.74	71.60
431.32	4.290	269.00	72.02
431.30	4.270	263.03	72.86
431.36	4.250	253.80	74.21
431.35	4.230	245.50	76.85
431.35	4.220	240.85	77.33
431.36	4.210	235.68	77.26
431.34	4.200	231.33	76.79
431.34	4.190	226.19	76.37
431.36	4.170	214.93	74.60
431.32	4.150	205.47	72.78
431.34	4.130	194.69	69.58
431.36	4.110	185.14	65.49
431.37	4.050	164.50	58.52
431.48	4.000	151.62	54.54
431.65	3.800	122.25	47.69
431.90	3.500	97.538	43.52
432.10	2.000	40.190	38.01
432.40	0.500	8.479	35.58

4. DATA ANALYSIS

The data analysis can be separated into three zones, the gaseous state, the liquid state, and the supercritical region ($T > T_c$).

4.1. The Gaseous State

From the data obtained we can derive dilute gas values ($P \rightarrow 0$) by extrapolation, at each temperature, of the data obtained at lower densities. The data obtained were found to have a quadratic temperature dependence and can be represented by

$$\lambda(0, T) = -6.41841 + 0.0420845T + 1.12871 \times 10^{-4}T^2 \qquad (5)$$

Table VII. Thermal Conductivity of n-Butane Near $T_{nom} = 436.0$ K ($\Delta T = 10.8 \pm 0.1$ K)

T (K)	P (MPa)	ρ (kg · m^{-3})	$\lambda(T, \rho)$ (mW · m^{-1} · K^{-1})
436.50	20.10	461.50	83.60
436.30	15.00	440.18	79.29
436.20	10.00	408.00	75.97
436.10	7.020	372.97	70.39
436.20	6.000	350.79	67.42
436.30	5.130	314.89	65.83
436.10	5.000	307.17	65.66
436.05	4.900	298.95	65.40
436.07	4.800	287.88	65.40
436.03	4.750	281.73	65.67
436.02	4.700	274.21	66.32
435.99	4.670	269.46	67.05
436.00	4.640	263.61	67.41
435.96	4.610	258.02	68.10
435.95	4.580	251.40	68.49
435.96	4.550	243.88	68.49
435.95	4.530	238.89	67.98
436.01	4.500	229.70	67.98
435.95	4.450	216.49	66.93
435.95	4.350	187.54	61.93
436.03	4.200	154.67	54.38
436.18	4.000	128.227	49.30
436.28	3.500	91.955	42.89
436.85	2.000	39.326	37.94
437.20	0.500	8.372	35.72

where λ is in mW · m^{-1} · K^{-1} and T is in K. Variance $\sigma = 0.22$ mW · m^{-1} · K (1.5% at lower temperatures and 0.4% at the higher temperatures). The extrapolated values are presented in Table XII and are shown in Fig. 1, together with the results obtained by other authors.

For temperatures below 400 K our values agree, within their mutual uncertainty, with the results of Ehya et al. [1], Kramer and Comings [2], and Parkinson and Gray [3]. However, our results depart considerably from the results of Ehya et al. [1] for higher temperatures, the difference in the two sets of results being of the order of 8% at 600 K if one considers the calculated value using their correlation (7a), which is far beyond the mutual uncertainty.

The isotherm at 601.2 K has been extensively studied in this work, and it can be easily seen from Fig. 4 of Ref. [1] that the experimental points all lie above the fitted curve for the range 500–700 K. The experimental method used by Ehya et al. is likely to have large errors at high tempera-

Table VIII. Thermal Conductivity of n-Butane at $T_{nom} = 454.2$ K ($\Delta T = 29.1 \pm 0.1$ K)

T (K)	P (MPa)	ρ (kg · m^{-3})	$\lambda(T, \rho)$ (mW · m^{-1} · K^{-1})	$\lambda(T_{nom}, \rho)$ (mW · m^{-1} · K^{-1})
454.3	70.10	542.91	112.1	112.1
454.3	59.90	530.01	106.7	106.7
454.3	50.00	515.38	102.9	102.9
454.7	40.00	497.16	96.21	96.15
454.5	30.00	474.25	92.44	92.40
454.4	20.00	441.00	84.22	84.19
454.5	14.00	408.84	76.56	76.52
454.5	10.00	372.26	72.13	72.09
454.3	7.000	310.87	66.61	
454.1	6.000	257.64	64.07	
454.2	5.800	240.47	62.32	
454.2	5.700	231.41	61.60	
454.2	5.600	221.88	61.03	
454.2	5.500	211.93	60.11	
453.4	5.000	164.84	52.95	53.05
453.4	4.000	98.519	45.69	45.79
453.6	2.000	36.685	39.81	39.88
453.8	0.485	7.775	37.72	37.77

Table IX. Thermal Conductivity of n-Butane at $T_{nom} = 480.0$ K ($\Delta T = 54.8 \pm 0.1$ K)

T (K)	P (MPa)	ρ (kg · m^{-3})	$\lambda(T, \rho)$ (mW · m^{-1} · K^{-1})	$\lambda(T_{nom}, \rho)$ (mW · m^{-1} · K^{-1})
479.6	70.00	527.63	109.3	109.3
479.4	60.00	514.08	105.6	105.7
479.6	50.00	497.81	100.4	100.5
479.6	40.00	477.96	95.66	95.72
480.1	30.00	451.33	87.51	87.50
480.0	20.00	411.62	80.68	80.68
480.0	14.00	369.90	74.02	74.02
480.0	10.00	314.76	68.43	68.43
479.9	8.50	275.52	65.13	65.14
479.9	7.50	236.52	62.34	62.35
480.1	7.25	224.31	61.09	61.08
479.0	7.00	215.25	60.24	60.39
479.0	6.00	161.49	54.52	54.67
478.9	5.00	115.20	51.44	51.58
479.0	4.00	80.834	47.29	47.43
479.0	3.00	54.681	43.82	43.85
479.1	2.00	33.512	42.46	42.58
479.3	0.485	7.316	40.76	40.85

Table X. Thermal Conductivity of n-Butane at $T_{nom} = 518.2$ K ($\Delta T = 93.0 \pm 0.1$ K)

T (K)	P (MPa)	ρ (kg · m^{-3})	$\lambda(T, \rho)$ (mW · m^{-1} · K^{-1})	$\lambda(T_{nom}, \rho)$ (mW · m^{-1} · K^{-1})
518.0	70.00	505.41	108.2	108.2
518.0	60.20	490.52	104.4	104.4
518.0	50.30	472.58	98.90	98.93
518.0	40.10	449.37	93.14	93.17
518.0	30.00	418.00	88.82	88.85
518.2	22.10	380.98	81.00	81.00
518.3	16.00	333.57	75.42	75.41
518.4	12.00	277.58	69.97	69.94
518.5	10.00	233.45	65.22	65.17
518.6	9.65	224.13	64.71	64.66
518.6	9.00	205.93	62.86	62.81
518.7	7.00	144.03	58.47	58.40
518.7	5.00	89.161	52.77	52.70
519.4	3.00	47.08	49.75	49.59
519.8	0.49	6.766	46.96	46.75

Table XI. Thermal Conductivity of n-Butane at $T_{nom} = 601.2$ K ($\Delta T = 176.0 \pm 0.1$K)

T (K)	P (MPa)	ρ (kg · m^{-3})	$\lambda(T, \rho)$ (mW · m^{-1} · K^{-1})	$\lambda(T_{nom}, \rho)$ (mW · m^{-1} · K^{-1})
601.0	69.90	460.92	107.1	107.1
601.0	60.00	442.79	103.3	103.3
601.0	50.00	420.45	98.62	98.66
601.0	40.00	391.61	93.70	93.74
601.0	30.00	350.82	87.40	87.44
601.0	25.00	321.96	84.32	84.34
601.4	20.00	282.67	80.16	80.12
601.6	16.00	239.69	76.08	76.01
601.6	14.83	224.62	74.77	74.70
601.5	13.00	198.44	72.89	72.84
601.3	13.00	198.60	72.83	72.81
601.9	10.00	148.88	69.48	69.36
601.3	8.000	114.79	67.16	67.14
602.3	7.015	97.969	65.74	64.84
601.9	6.500	89.722	64.91	64.79
602.3	5.000	66.309	63.43	63.23
602.4	4.000	51.676	62.69	62.48
602.7	3.005	37.819	61.58	61.31
602.3	2.000	24.556	61.48	61.28
602.2	2.000	24.561	61.26	61.08
602.2	1.000	11.966	60.67	60.49
602.7	0.500	5.898	60.28	60.01
602.8	0.500	5.897	60.02	59.74

Table XII. Zero Density Values of the Thermal Conductivity of n-Butane

T (K)	λ_0 (mW · m^{-1} · K^{-1})
298.2	16.2
358.2	23.0
383.2	26.6
413.2	30.2
426.0	31.8
427.4	31.9
480.0	40.0
518.2	45.8
601.2	59.7

tures, where the assumption of equal radiation and potential lead losses in vacuum and in the gas is no longer valid. The heat losses by potential leads at high temperatures must be less important in the gas than in vacuum because the thermal conductivity of the gas is very high. The results of Ehya et al. seem to be overcorrected for this effect. This fact explains the large discrepancy with our values.

The thermal conductivity of n-butane at low density can in principle be evaluated from the kinetic theory of dilute polyatomic gases. It is now known that inelastic collisions play a definite role in the overall thermal conductivity of dilute gases [14]. In the first order theory of Wang Chang et

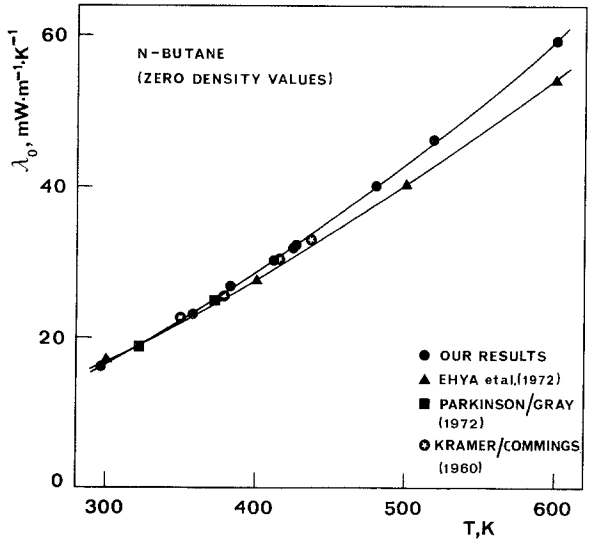

Fig. 1. Zero density values $\lambda_0 = \lambda(0, T)$ of the thermal conductivity of n-butane.

al. [15], the relationship between the viscosity of a gas η and its thermal conductivity may be written as follows:

$$\frac{M\lambda}{R\eta} = \frac{5}{2}\left(\frac{3}{2} - \Delta\right) + \frac{\rho D_{\text{int}}}{\eta}\left(\frac{C_{v_{\text{int}}}}{R} + \Delta\right) \tag{6}$$

with

$$\Delta = \frac{2C_{v_{\text{int}}}}{\pi\xi_{\text{int}}}\left[\frac{5}{2} - \frac{\rho D_{\text{int}}}{\eta}\right]\left[1 + \frac{2}{\pi\xi_{\text{int}}}\left(\frac{5}{3}\frac{C_{v_{\text{int}}}}{R} + \frac{\rho D_{\text{int}}}{\eta}\right)\right]^{-1} \tag{7}$$

In these equations, M is the molecular mass of the gas, $C_{v_{\text{int}}}$ is its internal heat capacity at constant volume, ρ is the mass density of the gas, ξ_{int} the collision number for internal energy relaxation, and D_{int} is the so-called diffusion coefficient for internal energy in the gas. When rotational and vibrational modes are present [16],

$$\frac{C_{v_{\text{int}}}}{\xi_{\text{int}}} = \frac{C_{v_{\text{rot}}}}{\xi_{\text{rot}}} + \frac{C_{v_{\text{vib}}}}{\xi_{\text{vib}}} \tag{8}$$

This theory neglects the spin polarization in the gas, but in the absence of data on the effect of magnetic fields in the thermal conductivity of n-butane, the correction to it must be neglected.

Maitland and coworkers [14] made an extensive study of the effect of inelastic collisions on the thermal conductivity of light gases, and we have applied here the same type of calculations. Following their suggestion, and using the results of first order kinetic theory, we can write

$$\frac{\rho D_{\text{int}}}{\eta} = \frac{\rho D}{\eta}\left(\frac{D_{\text{int}}}{D}\right) = \frac{6}{5}A^*\frac{D_{\text{int}}}{D} \tag{9}$$

where D is the self-diffusion coefficient of the gas, and A^* is the ratio of two collision integrals [17], which for elastic collisions can be evaluated from the expressions of the extended law of corresponding states [17].

Knowing the values of the viscocity of n-butane [18], we can use Eqs. (6)–(9) to obtain the locus of points of D_{int}/D as a function of A^* that reproduces the experimental values for the thermal conductivities. The heat capacities were taken from Ref. [13], while the collision numbers for rotational and vibration relaxation in butane have been taken from the monograph by Lambert [19]. The data presented in the monograph for n-butane refer only to $\xi_{\text{vib}} = 1.6$ at 300 K, and an estimate of $\xi_{\text{rot}} = 1.1$ was

made extrapolating the values found for ethane and propane. We have assumed, to a first approximation, that these values do not vary with temperature, as no data exist.

As neither D_{int}/D nor A^* can yet be obtained reliably from any independent source, we can only obtain its product and a locus of the pairs of values, necessary to reproduce the experimental data, allowing us to assess the magnitude of the effects of inelastic collisions. Figure 2 shows the locus of A^* and D_{int}/D points for 298 K and 468 K, and the contribution of inelastic collisions is evident if one compares the elastic values of A^* and D_{int}/D. For instance, if we use the value of A^* taken from the elastic formulae [17], we obtain for $T = 298$, $A^* \sim 1.137$; D_{int}/D should be ~ 0.95 in order to reproduce the experimental data. Conversely, if to D_{int}/D is given the value of unity, then A^* must be ~ 1.08, less than the value of 1.137 expected from elastic calculations. The behavior for 468 K is similar, although some care must be given to the interpretation as we have used collision numbers known for 300 K. If we use $D_{int} = D$ in Eq. (10) we can reproduce the data at 298 K with an error of 1%, but the departure at 468 K is as large as 6.4%. The results demonstrate that for butane, the inelastic collisions are not very frequent at room temperature, but they became very important at higher temperatures.

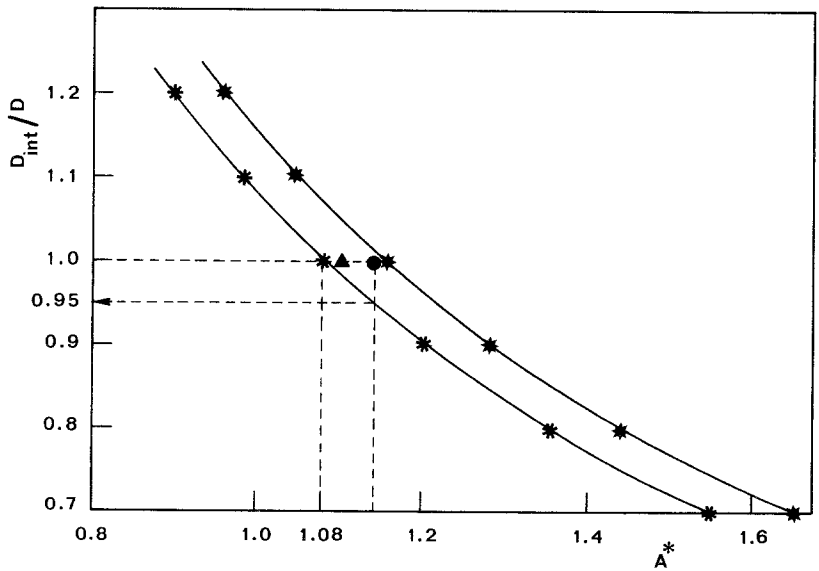

Fig. 2. Locus of points of D_{int}/D and A^* necessary to reproduce the experimental low density thermal conductivity data for n-butane at 298 K and 468 K. * 298K; ★ 468 K; ● elastic value; ▲ elastic value.

4.2. The Liquid State

The liquid state isotherms measured cover a range of states from 298.2 K to 413.2 K, saturation line to 70 MPa. This includes a density range of 350–650 kg · m^{-3}. The thermal conductivity excess defined by

$$\Delta\lambda(\rho, T) = \lambda(\rho, T) - \lambda(0, T) \tag{10}$$

is plotted in Fig. 3. This figure shows that all the points fit the same curve, i.e., the excess liquid thermal conductivity is a function of density alone in the temperature range considered. A cubic fit in density was selected to describe this variation; the equation is

$$\Delta\lambda = 58.430 - 8.1635 \times 10^{-2}\rho - 2.3034 \times 10^{-4}\rho^2 - 8.1645 \times 10^{-7}\rho^3 \tag{11}$$

with a variance of 0.67 mW · m^{-1} · K^{-1}, which corresponds to 1.2% at low

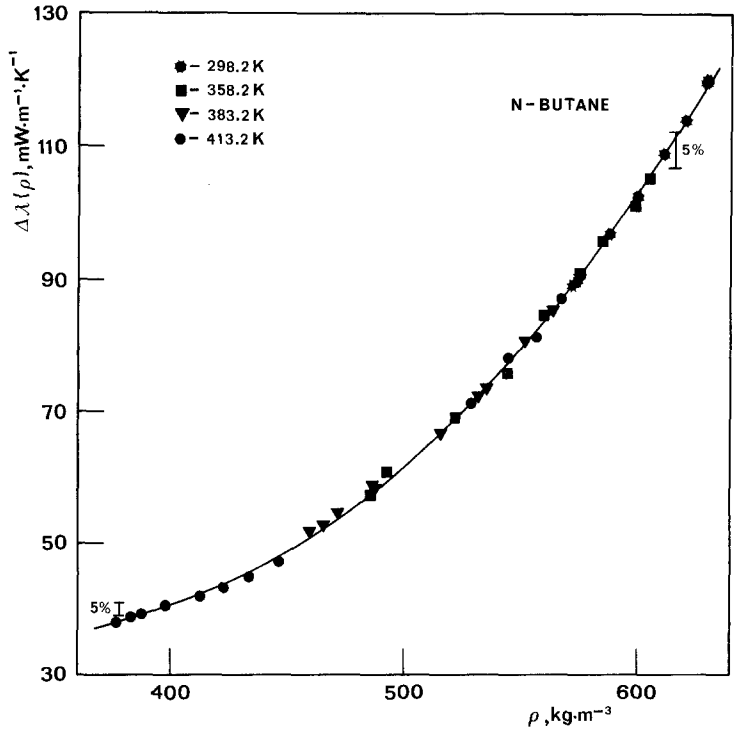

Fig. 3. The excess thermal conductivity of n-butane as a function of density. See key in figure for different temperatures.

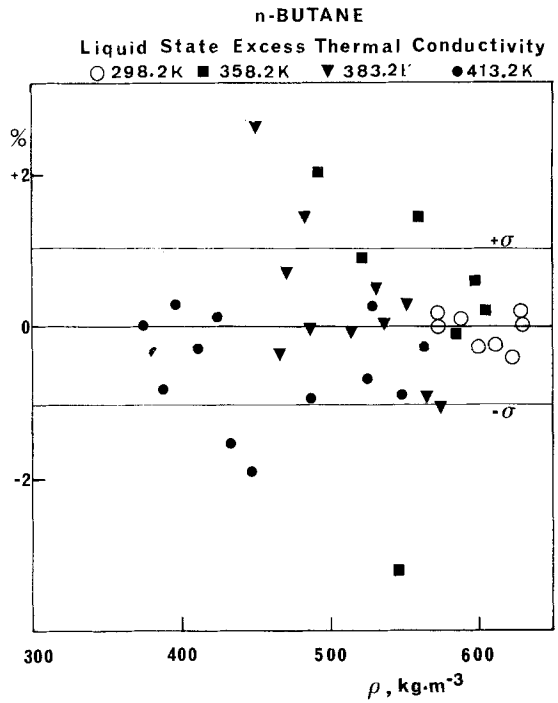

Fig. 4. Scattering diagram for Eq. (9). See key in figure for different temperatures.

density and 0.5% at high density. Figure 4 shows the scatter of the data for this fit, and it can be seen that the points mainly lie within the 2σ interval; no systematic variation was detected. The use of Eqs. (10) and (11) together with the values of λ_0 from Eq. (5) gives the value of the thermal conductivity for any density between 350 and 650 kg · m^{-3}.

The data now obtained can be compared with those of previous authors [2, 4, 5] by plotting the thermal conductivity as a function of pressure for various temperatures. The results of this comparison show that previous results do not agree very well. As an example we can say that the data by Kazaryan [5] and the data by Carmichael and Sage [4] at abut 375 K differ by 4%, and the latter differ by 13% with the data of Kramer and Comings [2]. Our results agree within 3% with Kazaryan's data at 298 K and 375 K, but at the latter temperature they differ as much as 6% from Carmichael and Sage's data (our results being greater) and 7% with Kramer and Comings' results (our results being smaller).

We can then conclude that our data (2% accuracy) agree with Kazaryan's data (5% accuracy) within their mutual uncertainty, and that

Kramer and Comings' data are about 7% greater than our data, which is far beyond the mutual uncertainty of the data. Carmichael and Sage's data [4] lie about 6% below our data and have about the same pressure coefficient as our data at the higher temperatures. We think therefore that our data are the most reliable presented so far and that for lower temperatures the data of Kazaryan [5] can be used.

4.3. The Supercritical Region

We have made an extensive experimental study in the supercritical region of n-butane, at seven different temperatures (pseudoisotherms near the critical point). The results are presented in Tables V to XI and, as far as we know, it is the first study in this region, although the data presented by Kramer and Comings [2] show some humps for $T_R = 1.03$, considered as a convection effect. In the supercritical region the thermal conductivity can be represented by an equation of the following type [21]:

$$\lambda(\rho, T) = \lambda(0, T) + \Delta\lambda(\rho, T) + \Delta\lambda_c(\rho, T) \tag{12}$$

where $\Delta\lambda_c(\rho, T)$ expresses the so-called critical enhancement. In this region, the temperature variation is very important, and the data can only be corrected for a nominal temperature far from the critical temperature ($T > 454.2$ K).

Figure 5 shows the complete data obtained, including the liquid and gas zone, as a function of density for all the investigated isotherms. The isotherms 428.8 K, 431.4 K, and 436.0 K should be more properly called pseudoisotherms as the temperature of each experimental datum does not always coincide with the nominal temperature. It can be easily shown that the critical enhancement is very large and that it is well-defined for all isotherms.

The isotherm at 601.2 K was tested in order to see if at this temperature we were far enough from the critical point to consider this isotherm as a completely critical "free" effect and obtain information about the background or "ideal" thermal conductivity, defined as the sum of $\lambda(0, T)$ and $\Delta\lambda(\rho, T)$ (see Eq. 12). The data for this isotherm has been fitted to a power series in density as the accuracy of the data did not justify a logarithmic term, and the result obtained was

$$\lambda(601.2\text{ K}) = 58.93 + 4.9984 \times 10^{-2}\rho + 1.4643 \times 10^{-4}\rho^2 - 5.243 \times 10^{-7}\rho^3 + 9.837 \times 10^{-10}\rho^4 \tag{13}$$

with a variance of 0.22 $\text{mW} \cdot \text{m}^{-1} \cdot \text{K}^{-1}$. The 4th order polynomial was

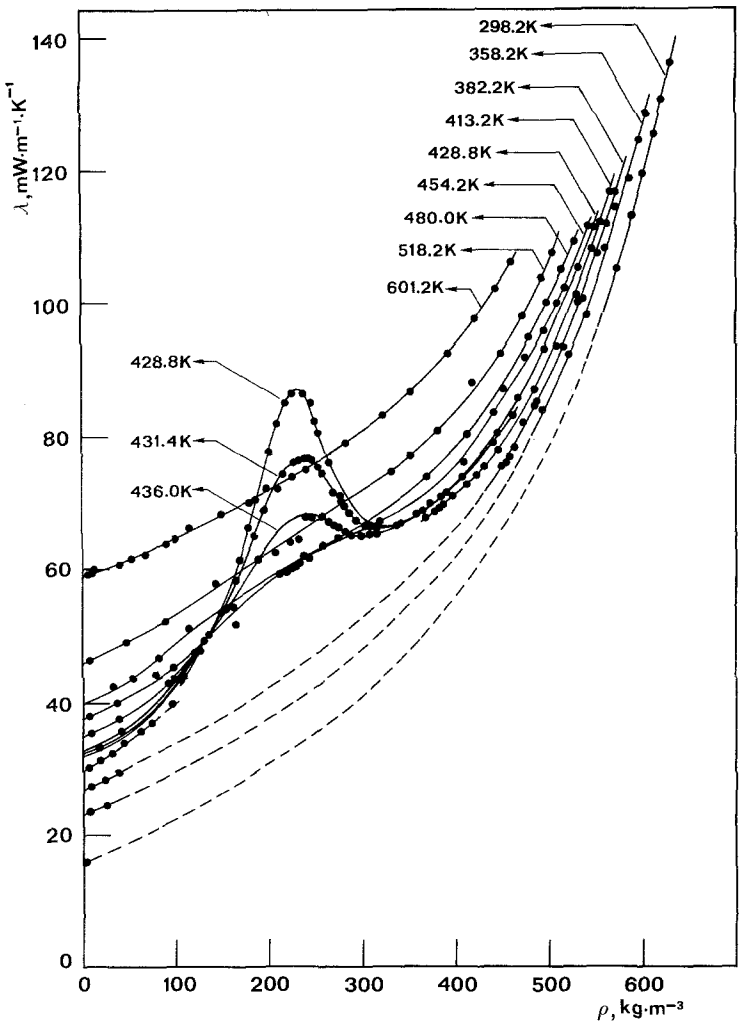

Fig. 5. The thermal conductivity of n-butane as a function of density and temperature. Experimental points.

chosen as no S-shaped scattering diagram was obtained and the variance being of the same order of the 5th and higher order fits, the lower order polynomial is the simplest to handle. If we compare the value of λ (0, 601.2 K) obtained from Eq. (15), 58.93 ± 0.22 mW $\cdot$ m^{-1} $\cdot$ K^{-1}, and compare it with the value of 59.7 mW $\cdot$ m^{-1} $\cdot$ K^{-1} obtained from graphical extrapolation, we can see that there is a small difference, mainly due to the lack of

some experimental data in the low density region. Nevertheless, the results agree within 1.2%.

If 58.93 is then subtracted from λ (601.2 K), we obtain the excess thermal conductivity for this temperature as a function of density. Thus at any other temperature we can obtain the ideal background thermal conductivity by simply adding $\lambda(0, T)$ for that temperature (Eq. 5 and Table XII) to the density dependence of Eq. (13), e.g.,

$$\lambda_{id}(\rho, T) = \lambda(0, T) + 4.9984 \times 10^{-2}\rho + 1.4643 \times 10^{-4}\rho^2 - 5.243 \times 10^{-7}\rho^3 + 9.837 \times 10^{-10}\rho^4 \quad (14)$$

We can now obtain $\Delta\lambda(\rho, T)$ by simply subtracting Eq. (12) from the measured thermal conductivity, Eq. (13):

$$\Delta\lambda_c(\rho, T) = \lambda_{\exp}(\rho, T) - \lambda_{id}(\rho, T) \quad (17)$$

Figure 6 shows the results obtained for the critical enhancement as a function of temperature and density; the peaks look fairly symmetric, although some "noise" in the high density range is found (about ± 3 $\text{mW} \cdot \text{m}^{-1} \cdot \text{K}^{-1}$). This behavior has already been found for fluids [10, 21], namely, for ethane, propane, and isobutane [10].

This critical enhancement can be treated, like other critical anomalies, as a function of the reduced temperature T^* and density ρ^* defined by Eqs. (16) and (17), whereas the reduced thermal conductivity is defined by Eq. (21):

$$T^* = \frac{T}{T_c} \quad (16)$$

$$\rho^* = \frac{\rho}{\rho_c} \quad (17)$$

$$\lambda^* = \lambda M^{1/2} T_c^{-1/2} \rho_c^{-2/3} R^{-3/2} \quad (18)$$

Using the values for $T_c = 425.16$ K, $\rho_c = 288$ kg $\cdot$ m^{-3}, and $M = 58.1243 \times 10^{-3}$ kg for butane [13], Eq. (20) can be written

$$\lambda^* = 1.961 \times 10^{-6}\lambda \quad (18a)$$

where λ must be expressed in $\text{W} \cdot \text{m}^{-1} \cdot \text{K}^{-1}$. Thus we can also define departure variables ΔT^* and $\Delta\rho^*$ as the difference between reduced ones

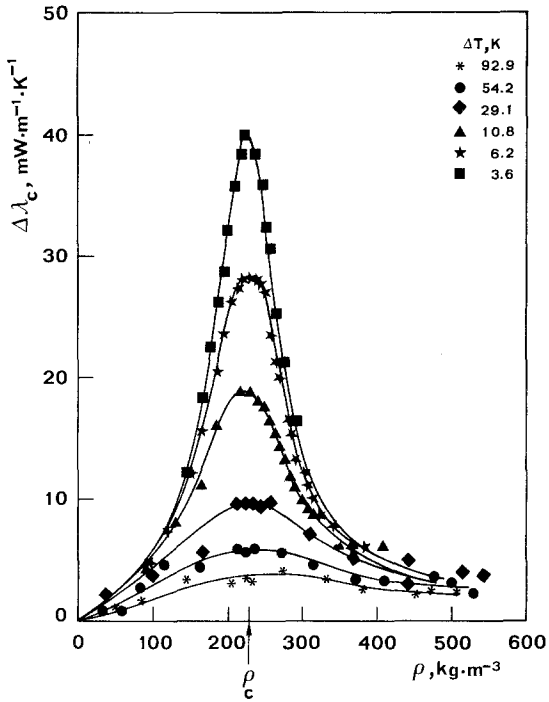

Fig. 6. The n-butane thermal conductivity critical enchancement. See key in figure for different temperatures.

and unity ($\Delta T^* = T^* - 1$, $\Delta\rho^* = \rho^* - 1$), the reduced critical enhancement being given by

$$\Delta\lambda_c^*(T^*, \rho^*) = 1.96 \times 10^{-6}\Delta\lambda_c(\rho, T) \tag{19}$$

In these variables the critical anomaly extends over a temperature range of $\Delta T^* \sim 1/3$ and a density range of $(\Delta\rho^*) \approx 2/3$, as was found previously for the lighter paraffins.

Following a discussion presented in a previous paper [10], it can be shown that along the critical isochore, $\Delta\lambda_c$ is proportional to the square root of isothermal compressibility. As the exponent governing the variation of K_T with temperature along the critical isochore is known to be 1.19 for $10^{-3} < \Delta T^* < 10^{-1}$, the exponent for $\Delta\lambda$ must be 0.595, a value which is close to the theoretical asymptotic value of -0.57. Figure 7 shows the values of $\Delta\lambda_c$ along the critical isochore ($\rho^* = 1$) as a function of ΔT^*, and it can be seen that the plot is not linear on a log scale. This has been already found for argon [12] and ethane, propane, and isobutane [10]. In

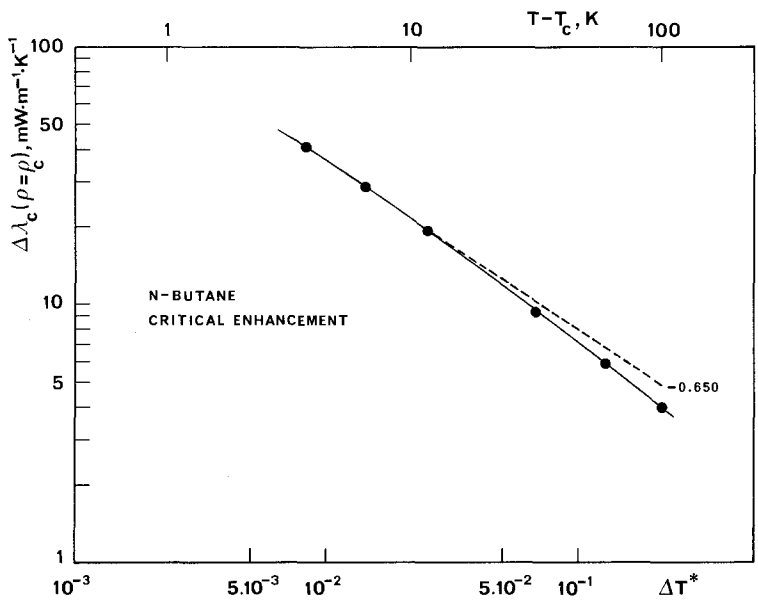

Fig. 7. The critical enchancement for the critical density as a function of the reduced departure temperature at ΔT^*. The dotted line shows values of slope of -0.650.

the interval 8×10^{-3} to 5×10^{-2} the slope is close to -0.65, a value already obtained for lighter paraffins.

We can then write that the thermal conductivity enhancement along the critical isochore varies with ΔT^* with a law of the type

$$\Delta\lambda_c = A(\Delta T^*)^{-\epsilon(\Delta T^*)} \tag{20}$$

where A is related to isothermal compressibility and other thermodynamic variables [10, 22], and the exponent ϵ is a function of ΔT^*. A reasonable description for $\epsilon(\Delta T^*)$ is

$$\epsilon = \epsilon_\infty(1 + 2.8\Delta T^*) \tag{21}$$

where ϵ_∞ is the theoretical asymptotic exponent for thermal conductivity ($+0.57$).

4.4. Comparative Study of the Thermal Conductivity of Light Hydrocarbons

It is now possible to make a comparative study of the behavior of C_1 to C_4 paraffins near the critical point, and in the dense gas region. Figure 8

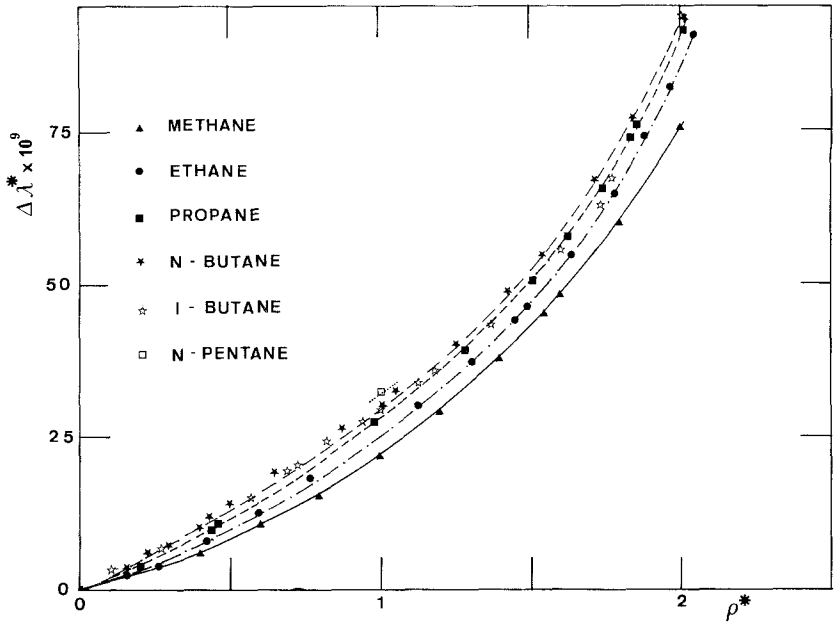

Fig. 8. The reduced excess thermal conductivity for different alkanes as a function of ρ^*. See key in figure for different alkane data.

shows the reduced excess thermal conductivity (using Eq. (18a) far from the critical region for methane, ethane, propane, and isobutane [10], n-butane (this work), and n-pentane using preliminary measurements [23]. We can see that the reduced excess thermal conductivity of n-alkanes is nonconformal, except for the same number of carbon atoms. The values for n-butane and isobutane seem to follow the same curve.

Again the tendency previously reported [10] for the increase of the first virial coefficient of the $\Delta\lambda^*(\rho^*)$ curve with molecular weight is confirmed with the n-butane and pentane results. The curve depends on ρ^* and on the particular hydrocarbon, and a corresponding states treatment using shape factors has to be applied. Predictions made using the corresponding states treatment formerly developed by Hanley [24] through the program TRAPP [25] shows that the thermal conductivity of n-butane in the liquid state is predicted within 0.5% of experimental values and that for the dense gas, the prediction is within 3%. We can then say that n-butane is conformal with methane, if the difference in shape is accounted for.

In the critical region some comparisons can be made. We present in Fig. 9 the reduced thermal conductivity enhancement along the critical isochore for the several hydrocarbons as functions of reduced temperature

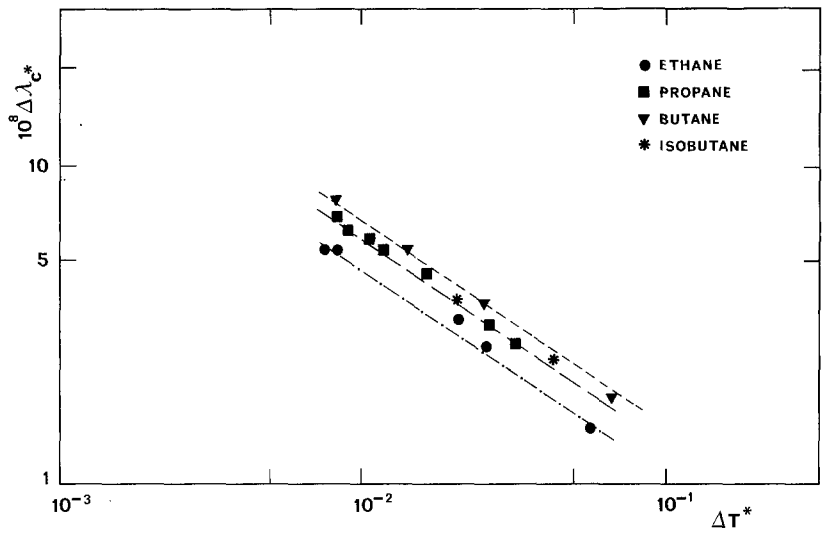

Fig. 9. The reduced thermal conductivity enhancement for the critical density as a function of ΔT^*, for different alkanes. See key in figure for different alkane data.

deviation. It can be seen that the critical behavior is slightly nonconformal from an absolute point of view, $\Delta\lambda^*$ increasing with the number of carbon atoms for the same ΔT^*. Nevertheless, the critical behavior dependence on ΔT^* confirms the universality of the exponent ϵ for all the hydrocarbons herein compared; the lines drawn in the figure are all parallel, corresponding to a slope of -0.65, which is the value found for n-butane for $\Delta T^* > 8 \times 10^{-3}$.

5. CONCLUSIONS

The thermal conductivity of n-butane has been measured for a wide range of thermodynamic states with an estimated overall accuracy of 2% with a steady-state concentric cylindrical apparatus. The liquid state, gaseous state, and supercritical fluid state have been covered. Comparisons with previous work shows the reliability and completeness of the present data.

The effect of the inelastic collisions on the dilute gas thermal conductivity has been studied, and it has been proved to be important. For the liquid state, it has been shown that the excess thermal conductivity is only a function of density and that for the supercritical region, the critical enhancement for n-butane behaves as for other fluids, the critical exponent being slightly temperature dependent.

A comparative study of the thermal conductivity of light hydrocarbons has also been made showing the conformality of the data if shape is taken into account for the excess thermal conductivity. The critical enhancement exponent has been found to be the same for all hydrocarbons, as expected.

ACKNOWLEDGMENTS

One of us (C. A. Nieto de Castro) wishes to thank Direcção Geral do Ensino Superior, Lisbon, Portugal, for a special grant that made possible the stay at the LIMHP-CNRS, Villetaneuse. We would like to thank Dr. W. A. Wakeham for several fruitful discussions, and Dr. H. M. Roder for the n-butane density calculations.

REFERENCES

1. H. Ehya, F. M. Faubert, and G. S. Springer, *Trans. ASME* 262 (1972).
2. F. R. Kramer and E. W. Comings, *J. Chem. Eng. Data* **5**:462 (1960).
3. C. Parkinson and P. Gray, *J. Chem. Soc., Farad. Trans.* **68**:1065 (1972).
4. L. T. Carmichael and B. H. Sage, *J. Chem. Eng. Data* **9**:511 (1964).
5. V. A. Kazaryan, *Gazov. Prom.* **15**:47 (1970).
6. J. F. T. Pittman, Ph.D. Thesis, Imperial College, London (1968).
7. V. P. Brykov, G. Kh. Mukhamedzyanov, and A. G. Usmanov, *Inzh-fiz. Zh.* **18**:82 (1970).
8. B. Le Neindre, Thesis, Université Paris VI (1969).
9. R. Tufeu, Thesis, Université Paris VI (1971).
10. R. Tufeu and B. Le Neindre, *High Temp.-High Press.* **13**:31 (1981).
11. M. N. Ozisik, *Radiative Transfer* (Wiley-Interscience, New York, 1973).
12. C. A. Nieto de Castro, H. M. Roder, *J. Res. Natl. Bur. Stds.* **86**:293 (1981).
13. W. M. Haynes and R. D. Goodwin, NBS Monograph 169 (1982).
14. G. C. Maitland, M. Mustafa, and W. A. Wakeham, *J. Chem. Soc. Farad. Trans. I* **79**:163 (1982).
15. C. S. Wang Chang, G. E. Uhlenbeck, and J. de Boer, in *Studies in Statistical Mechanics*, J. de Boer and G. E. Uhlenbeck, eds. (North Holland, Amsterdam) (1964) Vol. 2, part C.
16. L. Monchick, A. N. G. Pereira, and E. A. Mason, *J. Chem. Phys.* **42**:3241 (1965).
17. G. C. Maitland, M. Rigby, E. B. Smith, and W. A. Wakeham, *Intermolecular Forces: Their Origin and Determination* (Clarendon, Oxford, 1981).
18. Y. Abe, J. Kestin, H. E. Kalifa, and W. A. Wakeham, *Physica* **97A**:296 (1979).
19. J. D. Lambert, *Vibrational and Rotational Relaxation in Gases* (Clarendon, Oxford, 1977).
20. J. Kestin, R. Paul, A. A. Clifford, and W. A. Wakeham, *Physica* **100A**:349 (1980).
21. C. A. Nieto de Castro and H. M. Roder, in *Proc. 8th Symp. Thermophys. Properties*, J. V. Sengers, ed. (ASME, New York, 1982), Vol. I, p. 241.
22. H. J. M. Hanley, J. V. Sengers, and J. Ely, *Proc. 14th Int. Conf. Thermal Conductivity*, P. G. Klemens and T. K. Chu, eds. (Plenum, New York, 1976), p. 383.
23. R. Tufeu and B. Le Neindre (to be published).
24. H. J. M. Hanley, *Proc. 7th Symp. Thermophys. Properties*, A. Cezairliyan, ed. (ASME, New York, 1977), p. 668.
25. H. J. M. Hanley, NBS Technical Note 1039 (1981).